A precise method to determine the angular distribution of backscattered light to high angles

P. Gross, a) M. Störzer, S. Fiebig, M. Clausen, b) G. Maret, and C. M. Aegerter Fachbereich Physik, University of Konstanz, Box M621, 78457 Konstanz, Germany

(Received 11 December 2006; accepted 7 February 2007; published online 15 March 2007)

We present an approach to measure the angular dependence of the diffusely scattered intensity of a multiple scattering sample in backscattering geometry. Increasing scattering strength give rise to an increased width of the coherent backscattering and sets higher demands on the angular detection range. This is of particular interest in the search for the transition to Anderson localization of light. To cover a range of -60° to $+85^{\circ}$ from direct back-reflection, we introduced a new parallel intensity recording technique. This allows one-shot measurements, with fast alignment and short measuring time, which prevents the influence of illumination variations. Configurational average is achieved by rotating the sample and singly scattered light is suppressed with the use of circularly polarized light up to 97%. This implies that backscattering enhancements of almost two can be achieved. In combination with a standard setup for measuring small angles up to $\pm 3^{\circ}$, a full characterization of the coherent backscattering cone can be achieved. With this setup we are able to accurately determine transport mean free paths as low as 235 nm. © 2007 American Institute of Physics.

[DOI: 10.1063/1.2712943]

I. INTRODUCTION

In the characterization of (sub-)micron sized particles, light scattering is very commonly used. The use of multiangle setups in this realm, where the scattered light is detected at several forward angles simultaneously, has in the past lead to great improvements in accuracy and useability. In the investigation of turbid media, the light scattered back to the source is more important. This is because in that case multiple scattering leads to an enhancement of the intensity in the back direction as discussed below. The width of this enhancement of coherent backscattering around the direct backscattering direction is a very useful tool, because the key quantity, the transport mean free path l^* , is inversely proportional to this width and can hence be directly measured. From the transport mean free path, microscopic properties about the scatterers can then be inferred.² If the medium becomes increasingly turbid, the angular width of the backscattering enhancement becomes wider. Thus in the characterization of very turbid media, such as candidates^{3,4} for the observation of Anderson localization of photons, ^{5,6} a large angular region has to be covered by a backscattering measurement for reliable estimates of l^* . This is mainly due to the fact that a proper determination of the incoherent diffuse background is vital for a reliable estimate of the full width at half maximum (FWHM) and hence l^* . Here we present the development and test of a set-up which is capable of determining the intensity of backscattered light to angles of up to 85°. Due to the use of a simultaneous measurement

In the following, we will give a brief introduction to coherent backscattering measurements and discuss previous setups with which to determine l^* of turbid samples in Sec. I. Section II will then describe our new setup in detail, while Sec. III presents some results of the characterization of very turbid samples.

A. Coherent backscattering

When a semi-infinite, disordered sample is illuminated with a light source, all of the light will be reflected from the sample after performing a random walk inside it. Looking at the paths that lead to direct back-reflection, each of these light paths has a counterpart that visits the same scatterers, but in reverse order. Thus the path and its counterpart have the same length and, therefore, a phase difference of zero. This leads to constructive interference of photons on these paths and hence to a twofold enhancement of the intensity in direct back-reflection with respect to the incoherent background. If the detection angle is tilted away from the backreflection direction, a phase difference is introduced, which depends on the distance of the points of entry and exit of the light in analogy to a two slit experiment. Averaging over all possible end-to-end distances, one obtains a distribution of intensity with the backscattering angle, which decreases with increasing angle from a value of twice the incoherent background at zero angle to the incoherent background at higher angles. The width of this decrease is given by the inverse of the product of the mean free path l^* with the wave number kof the incident radiation. From this theoretical description of

for all angles, difficulties stemming from illumination variations, lengthy alignment, etc. can be circumvented. Furthermore, due to the calibration method, the angular dependence of the incoherent background is directly taken into account and only the coherent signal is measured.

a)Present address: Vrije Universiteit Amsterdam, De Boelelaan 1081, 1081HV Amsterdam, The Netherlands.

b) Present address: Universität Münster, Schlossplatz 5, 48149 Münster, Germany.

c)Electronic mail: christof.aegerter@uni-konstanz.de

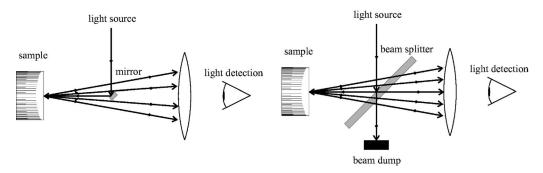


FIG. 1. Principle of a setup to measure the backscattering cone using a mirror (left) or a beam splitter (right). The sample is illuminated with a spatially broadened laser. In contrast to the setup using a mirror, the beam splitter setup allows the measurement of the intensity in direct back-reflection, however, needs a beam dump. The positive lens collects the light, which is then recorded with, e.g., a CCD-camera.

the shape of the CBC, it can be obtained that its FWHM is inversely proportional to kl^* with a proportionality constant very close to one. In all of the above, averaging over the disorder in the sample is important, as in each realization of the disorder there are random phase differences leading to a strongly varying intensity pattern called a speckle pattern. The speckle pattern is averaged out by rotating the sample for solid powders or by particle diffusion for samples in solution.

As described above, the shape of the CBC is determined solely by the ratio of the wavelength and the transport mean free path, however, the value of the enhancement factor also depends on the polarization used.^{2,8} This is due to the fact that depending on the polarization, singly scattered light can give a contribution to the incoherent background, thus leading to an overestimation of its height. When using circular polarization however, singly scattered light can be completely suppressed, such that the enhancement factor can be measured at its maximum value of two. Thus, setups to accurately measure the CBC have to efficiently reduce stray light as well as contributions from singly scattered light using circular polarization. This is usually done by a combination of a linear polarizer (LP) and a quarter wave plate (QWP) in both the incident and detected light. Thus, the light hitting the sample is circularly polarized with a given helicity. Singly scattered light can be treated as reflected light and hence will have the opposite helicity to the incident light. The combination QWP and LP in front of the detector will thus be crossed with respect to singly scattered light and only the unpolarized, incoherent background of the diffusive light will be detected. However, due to the nature of the QWP, such a setup is only possible at very limited wavelengths and with light incident perpendicular to the QWP as discussed below.

B. Former setup designs

To measure the CBC one must record the angular dependence of the back-scattered light of a light source that illuminates the sample. If an incoherent light source were used, polarization effects as well as wavelength averaging would lead to a misrepresentation of the background and thus the CBC, such that experimental investigations in the past have always relied on the use of a coherent light source. However, a CBC can also be observed with incoherent white light.

These existing setups have used a mirror⁹ beam-splitter^{10,11} to come very close to the direct backreflection. The two methods are illustrated in Fig. 1. Incident light is reflected onto the sample either by a mirror or a beam-splitter and the intensity is observed at angles near backscattering. This is done either by using a charge coupled device (CCD) camera covering the two-dimensional intensity distribution or by focusing the light onto a fiber and a photomultiplier tube (PMT) which is scanned over angles. In contrast to the beam-splitter, the mirror casts a shadow close to the direction of back-reflection depending on its size. Therefore, close to back reflection, a mirror setup cannot be used and a beam splitter has the strong advantage that the whole range of angles close to zero can be investigated. However, similar to the mirror setup, there is the drawback that usually only very limited angular regions can be covered. This is because the backscattered light has to be imaged either onto the CCD camera or the PMT. Thus the corresponding optics has to cover the angular range of interest without distortions. This is usually limited by the size of available lenses to a range of $\pm 2^{\circ}-3^{\circ}$. This problem can be avoided by using a movable fiber, which scans the angular dependence of the backscattered light. 11,12 In this case, care has to be taken that the recorded light always passes the polarization filter (and QWP, see below) at right angles, such that singly scattered light can be efficiently and homogeneously reduced. Otherwise the polarization properties will change, leading to a misestimation of the incoherent background and hence a distortion of the CBC. In order to still be able to measure close to direct back reflection, Wiersma et al. 11 have used a setup, where a beam splitter and a fiber are rotated off-center, while the sample rotation is compensated. With this method it is possible to extend the angular detection range, which then has the detection limits of -6° to 20° , while still having high angular resolution close to the center of the CBC. Alternatively, Tweer¹² used a movable fiber with a QWP directly in front and illumination without a beamsplitter. This setup has an angular range of 35° only in the positive direction and cannot resolve a zero angle. Both of these methods with movable fibers are slow in data acquisition, as each position has to be scanned in turn. Furthermore, alignment of the different parts is hampered by the fact that the CBC has to be scanned before a new alignment can be made.

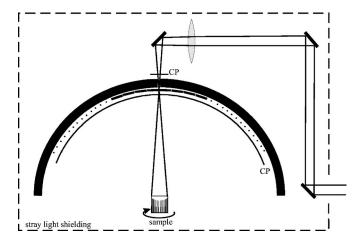


FIG. 2. Illustration of the setup to measure the backscattered light up to high angles. 256 photodiodes are mounted on a detection arc with a diameter of 1.2 m. The arc is set up horizontally, so that the sample can be placed upright. Close to the back-reflection, eight photodiode arrays are positioned as indicated by the black lines are distributed. The photodiodes at higher angles are indicated by black dots. A positive lens produces divergent light, and a focal point in the plain of the detectors 0.6 m distant from the sample. The whole setup is put in a black box to shield stray light. The combination of two circular polarizing foils (CP), is used to suppress singly scattered light.

When studying very strong scattering, which is required to come close to the predicted Anderson localization⁶ for multiple scattering of light, the CBC are expected to be increasingly broad. A quick estimate of the width of such candidate cones can be done using the Ioffe-Regel criterion.¹³ In that case the transition to Anderson localization would take place at $kl^* \simeq 1$. Thus the FWHM as calculated above would turn out to be $\approx 60^{\circ}$, far beyond the capabilities of existing setups. This is, however, an overestimation of the FWHM as reflections at the sample surface due to the change in refractive index between the scattering medium and vacuum will lead to a narrowing of the CBC. ¹⁴ Given the fact that in order to reach the necessary small l^* one needs very strong scattering samples with a high refractive index (exceeding 2.5) at packing fractions of \sim 40%. Therefore, the sample will have an effective refractive index of ≈ 1.5 , 15 which gives rise to significant reflections at the sample surface. This in turn leads to a reduction in the FWHM to about 20° close to the Anderson transition. As the incoherent background has to be measured accurately for a proper determination of the CBC, even such a narrower estimate still means that existing setups cannot be used to resolved CBCs close to the transition to Anderson localization. Furthermore, extending the angular detection range of a setup using a movable fiber also has the drawback that measurement time and alignment difficulty increase steadily, such that the setup is vulnerable to changes of the experimental condition such as laser drifts.

Due to the difficulties of the existing methods of measuring the CBC, we have devised a new technique to record the backscattered light with a high angular detection range and sufficient angular resolution in a one-shot measurement.

II. EXPERIMENTAL SETUP

Our newly constructed wide angle coherent backscattering setup, which is shown schematically in Fig. 2, uses 256

photodiodes to determine the intensity at a fixed angle simultaneously. To investigate the backscattering cone it is necessary to average over speckles, since the intensity fluctuations of the speckle pattern are much larger than the enhancement of the backscattering cone. Therefore, the sample is rotated around the axis normal to the surface of the sample. For a sufficient measurement duration and small speckle spots, the speckle pattern averages out, and the typical backscattering cone with an incoherent background remains.

To resolve the angular regime close to back-reflection, a high angular resolution was desired. Therefore, we use photodiode arrays, ¹⁶ which consist of 16 low-noise photodiodes which are separated by about 1.5 mm. Due to the fact that the minimum distance between two photodiodes is predetermined, the angular resolution is given by the diameter of the detection arc. Here a compromise between angular resolution and signal strength had to be found. We used a diameter of 1.2 m, which yields an angular resolution of 0.15° close to the direction of back-reflection. For higher angles the expected gradient of the backscattering cone is smaller, and one approaches the region where the intensity is dominated by incoherent scattering. Therefore, a lower angular resolution is sufficient. Here we used single photodiodes. ¹⁷ The achieved angular resolution is 0.15° from ±0.15° to ±9.75°, 0.7° from $\pm 9.75^{\circ}$ to $\pm 19.55^{\circ}$, 1° from $\pm 19.55^{\circ}$ to $\pm 60^{\circ}$, and finally 3° for angles between 60° and 85°. The arc and the sample are situated inside a stray light shielding to ensure that only light from the sample reaches the photodiodes. This is crucial since all stray light collected by the photodiodes would give contributions to the incoherent background and, therefore, reduce the coherent backscattering enhancement.

Both types of photodetectors have a quantum efficiency of 0.35 at 600 nm and a dark current of the order of 1 pA. This is essential to provide a good signal-to-noise ratio. The setup was designed so that the photocurrent of the diodes has a signal to noise ratio of the order of 1000 for an incident laser power of 0.5 W. This corresponds to an intensity at the photodiodes of $\approx 0.5 \mu W$. The low-noise photocurrent is amplified and processed using custom designed circuits, to end up with low-noise data. The circuits operate as follows: First for each photodiode, the corresponding switched integrator ¹⁸ amplifies the signal, which then is digitized by the AD converter. ¹⁹ An 8-bit microcontroller ²⁰ collects and stores the obtained data in two words of the microcontroller, such that effectively a 16-bit resolution is obtained. The microcontroller also runs the measuring algorithm. The timing of this algorithm gives the length of the whole measurement, which is typically of the order of one second. Due to the fact that all photodiodes start the light detection simultaneously, laser drifts, background illumination, vibrations, and other origins of time dependent illumination changes do not affect the measurement.

A. Polarization in multiple scattering

As mentioned before, the CBC is an interference effect. In the absence of a magnetic field, the polarization on two time-inverted paths will map, such that interference is possible.²¹ This is not necessarily the case for other paths constituting the incoherent background, which leads to a fac-

tor of two in the enhancement. For a maximum contrast of the CBC over the incoherent background, it is crucial to suppress the singly scattered light. This is because these photons have no time-inverted counterpart and hence lead to an overestimation of the incoherent background. By using the polarization conserving channel of circularly polarized light, single scattering is effectively cancelled out as a single reflection leads to a change in helicity of the photon. Therefore all of the measured intensity has paths contributing to the CBC and hence an enhancement of two can be measured. 11 However, as mentioned above, the usual setup with a LP in front of a QWP has its drawbacks due to the fact that a QWP is only effective in a very small wavelength window, and light has to be incident perpendicular on to QWP in order to produce proper circularly polarized light. This leads to great difficulties in setting up a one-shot measurement over large angular ranges and in the past only movable experiments with their specific drawbacks (such as long counting time and difficult alignment) have been carried out.

We circumvent this problem by using a circularly polarizing foil (CP) from 3M,²² which consists of two layers and, therefore, combines the effects of a LP and a QWP. This foil is bendable and its optical properties are very robust under wavelength changes. The first foil is placed behind the last mirror to obtain circularly polarized light. In front of the photodiodes we placed another CP, which follows the arc where the photodiodes are mounted, such that light is always incident perpendicular. With this arrangement we can suppress singly scattered light by 97%, which was verified with the help of a mirror in the sample position. The further advantage of the CP is that the single scattering suppression factor is wavelength independent from 580 to 620 nm. Thus our setup can be used to measure accurate CBCs in the wavelength region supplied by our dye laser.²³

B. Calibration

In order to obtain proper intensity measurements from our setup, each of the 256 photodiodes has to be calibrated. For this we have used a rotating block of teflon with a diameter of 4 cm and a thickness of 5 cm. Teflon has a transport mean free path of \approx 300 μ m and hence the CBC of teflon at a wavelength of 590 nm has a FWHM of about 0.02°. 24 This implies that with our setup teflon can be considered to give a purely incoherent signal since the CBC is much narrower than our angular resolution. We have measured the response of all photodiodes at 15 different incident laser powers, which are determined independently with a calibrated photodiode. The characteristic response of ten of the photodiodes is shown in Fig. 3, where it can be seen that they are quite linear over the whole range of intensities studied. The counts here refer to the response of the AD converter. In order to interpolate between the calibration measurements, a polynomial of second-order was fitted to each response curve, which is then used in subsequent measurements. This method of calibration also means that the angular dependence of the incoherent background as $cos(\theta)$, known as the Lambert-Beer distribution²⁵ is already taken into account in the calibration. This is because the angular dependence of the

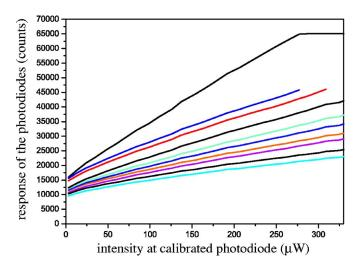


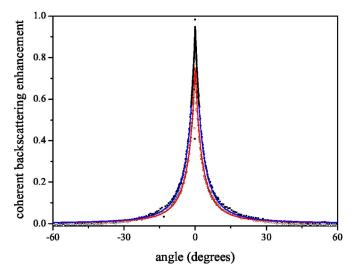
FIG. 3. The response of ten typical photodiodes against the intensity of the incident laser. The curves show the same characteristic with a difference in the gradient. This is due to the fact that the diodes differ in the detection angle and hence see a different part of the $\cos(\theta)$ background.

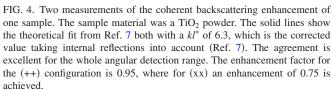
background is measured by the photodiodes, but all channels are calibrated to the incident intensity.

For each measurement, we furthermore take a reference measurement with the same teflon block used in the calibration. This allows us to subtract the incoherent background more precisely. Therefore, our data will only show the enhancement itself, such that the ideal value for the enhancement will be one. For full precision of the CBC determination, however, the different albedos of the sample and the reference have to be taken into account as well. In both cases, absorbtion is negligible, so the difference in albedo will arise from a small residual transmission through the sample (or reference) due to its finite extent. As noted above, the dimensions of the teflon reference sample are about $130 \times 130 \times 170$ in units of l^* . This implies that about 3% of the incoming intensity are lost leading to an albedo of 97%. As we will see below, our sample typically have dimensions of $10^5 \times 10^5 \times 10^4$ in units of l^* , such that they have an albedo of 99.99%. The difference of 3% in the reference would lead to an overestimation of the incoherent background in the sample by these 3% which is, therefore, subtracted manually.

III. RESULTS

To test our setup, we have used samples of ground ${\rm TiO_2}$. Due to its high refractive index (of 2.7 at 590 nm) and low absorption, such particles are ideal candidates for obtaining small values of kl^* . In Fig. 4, we show data for a sample consisting of particles of an average diameter of 540 nm with a polydispersity of 25%. To show the dependence on the incoming polarization, the figure shows measurements with both linear (xx) and circular (++) polarization in the polarization conserving channel. As can be seen, the enhancement factor is very different for the two, resulting in 0.95 for circular polarization and 0.75 for linearly polarized light. This is obtained from a fit to the theoretical calculation in the diffusion approximation allowing for different enhancement factors, which yields a value of l^* =590(20) nm. In the two





fits, the value of kl^* is constrained to be the same, showing that the shape of the CBC does indeed solely depend on this quantity.

The fact that the two measurements seem to have a different width is due to the fact that kl^* is given by the FWHM, which in turn is dependent on the value of the enhancement factor. However, the very good agreement of both measurements with the theory for the same kl^* shows the quality of the measurements. The lower enhancement factor in the case of linearly polarized light can be estimated from the back-scattering probability of Mie-spheres corresponding to our samples. Using far-field Mie scattering software to calculate this, we obtain a reduction factor of 20 to 30% in good agreement with the results of Fig. 4.

In order to determine the behavior at small angles, we employ a method using a beam-splitter and a CCD camera as discussed above. 10,12 Our setup uses a lens with a focal distance of 0.1 m which is also the distance between the lens and the CCD chip. The CCD chip has a resolution of 512 ×512 pixels, which in this setup results in an angular resolution of 0.012° over a range of ±3°. The drawback of a beam splitter method with highly scattering samples with very wide CBCs is that the background level and hence the enhancement cannot be determined due to the lack of angular range. Our setup, however, uses the same sample holders and polarization foil as well as stray light shielding in order to ensure the same physical situation as the wide angle setup. This implies that the overlap between the beam splitter setup and the wide angle setup can be used to adjust the intensity scale of the CCD chip to the calibrated wide angle data. An indication of this can be seen in the inset to Fig. 5, where the small angle part and the overlap of the different setups is shown. This combination gives enough resolution to observe the very tip of the cone and at the same time obtain a good estimate of the CBC enhancement.

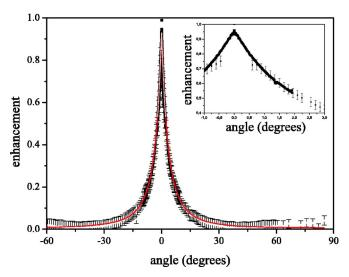


FIG. 5. Measurement of a sample with $kl^*=2.5$ with angles up to 85°. As can be seen, an enhancement of 0.95 is observed and the cone shape is reasonably well described by the theory of Akkermans *et al.*⁷ over the full angular range. The inset shows a magnification around small angles, where the wide angle setup overlaps with the small angle setup in order to determine the enhancement.

We have also measured other samples with average diameters of, e.g., 250 nm, which have yielded values of $l^*=235(25)$ nm, much lower than the wavelength and hence good candidates for the observation of Anderson localization.⁴ An example of this is shown in Fig. 5, where it can be seen that even for such strongly scattering systems we observe large enhancements of roughly 0.95 and CBCs which can be well-described by the theory of Akkermans et al. The reduction in enhancement arises mainly from the fact that the polarization foil only reduces single scattering by 97%. The rest of the reduction in enhancement can most likely be explained by the residual stray light and reflections from the shielding box. These can be estimated from teflon measurements to give an uncertainty of the order of one percent. Finally, for turbid samples, such as ours, recurrent multiple scattering has been proposed to also lead to a reduction in enhancement, 28 however, in our case this effect seems to be very small.

In conclusion wide angle apparatus allows sensitive measurements of the backscattering cone up to high detection angles on both sides of the cone with a very good enhancement. Additionally, due to the parallel intensity recording technique the setup is not affected by laser drifts and mechanical instabilities. Wavelength dependent measurements can be performed because the circular polarization foil used is wavelength independent in the window available to our dye laser.

ACKNOWLEDGMENTS

This work was supported by the Deutsche Forschungsgemeinschaft, the International Research and Training Group "Soft Condensed Matter of Model Systems," and the Center for Applied Photonics (CAP) at the University of Konstanz. The authors would also like to thank Christian Ortolf for support with the circuit design.

- ¹H. R. Haller, C. Destor, and D. S. Cannell, Rev. Sci. Instrum. **54**, 973 (1983).
- ² R. Lenke and G. Maret, in *Scattering in Polymeric and Colloidal Systems*, edited by W. Brown and K. Mortensen (Gordon and Breach Scientific, New York, 2000), Chap. 1.
- ³S. Eiden and G. Maret, J. Colloid Interface Sci. **250**, 281 (2002).
- ⁴ M. Störzer, P. Gross, C. M. Aegerter, and G. Maret, Phys. Rev. Lett. **96**, 063904 (2006).
- ⁵S. John, Phys. Rev. Lett. **58**, 2486 (1987).
- ⁶P. W. Anderson, Philos. Mag. B **52**, 505 (1985).
- ⁷E. Akkermans, P. E. Wolf, and R. Maynard, Phys. Rev. Lett. **56**, 1471 (1986).
- ⁸ M. I. Mishchenko, J. Opt. Soc. Am. A **9**, 978 (1992).
- ⁹P. E. Wolf and G. Maret, Phys. Rev. Lett. **55**, 2696 (1985).
- ¹⁰M. P. Van Albada and A. Lagedijk, Phys. Rev. Lett. 55, 2692 (1985).
- ¹¹ D. S. Wiersma, M. P. van Albada, and A. Lagendijk, Rev. Sci. Instrum. 66, 5473 (1995).
- ¹² R. Lenke, R. Tweer, and G. Maret, J. Opt. Soc. Am. A 4, 293 (2002); R. Tweer, Ph.D. thesis, Univ. of Konstanz (2002).
- ¹³ A. F. Ioffe and A. R. Regel, Prog. Semicond. **4**, 237 (1960).

- ¹⁴ J. X. Zhu, D. J. Pine, and D. A. Weitz, Phys. Rev. A. **44**, 3948 (1991).
- ¹⁵J. C. M. Garnett, Philos. Trans. R. Soc. London, Ser. A **203**, 385 (1904).
- ¹⁶Hamamatsu, S5668.
- ¹⁷Hamamatsu, S4011.
- ¹⁸Texas Instruments, IVC102.
- ¹⁹Texas Instruments, ADS8345 and ADS8344.
- ²⁰ ATMEL, AT89S8252.
- ²¹ F. Erbacher, R. Lenke, and G. Maret, Europhys. Lett. **21**, 551 (1993).
- ²²3M, J53-333, made from Cellulose Acetate Butyrate.
- ²³ Our setup consists of a Rhodamin 6G dye laser (Coherent 699) pumped by an Ar⁺ Laser (Coherent Innova 400) producing pulses with a width of \sim 20 ps at a wavelength of 590 nm.
- ²⁴D. S. Wiersma, Ph.D. thesis, Univ. of Amsterdam (1995).
- ²⁵ M. Born and E. Wolf, *Principles of Optics* (Pergamon, Oxford, 1980), 6th ed.
- ²⁶G. Mie, Ann. Phys. **25**, 377 (1908).
- ²⁷LightLab, Far-field Miescattering version 1.0 (Valley Scientific Inc., 1998)
- ²⁸ D. S. Wiersma, M. P. van Albada, B. A. van Tiggelen, and A. Lagendijk, Phys. Rev. Lett. **74**, 4193 (1995).